PAPER

Morphological impact of insulator on inkjet-printed transistor

Flexible and Printed Electronics

PAPER

Morphological impact of insulator on inkjet-printed transistor

Sjeung Jae Moon[1,2], **Malo Robin**[1,3], **Kuai Wenlin**[1], **Molard Yann**[3], **Byung Seong Bae**[2], **Tayeb Mohammed-Brahim**[1], **Emmanuel Jacques**[1,4] **and Maxime Harnois**[1,4]

[1] Institut d'Électronique et des Télécommunications de Rennes, Université Rennes 1, UMR CNRS 6164, Campus de Beaulieu, 35042 Rennes Cedex, France
[2] Department of Display Engineering, Hoseo University, Asan, Chungnam 336-795, Republic of Korea
[3] Institut des Sciences Chimiques de Rennes, Université de Rennes 1, CNRS UMR 6226, Rennes, France
[4] Authors to whom any correspondence should be addressed.

E-mail: maxime.harnois@univ-rennes1.fr

RECEIVED
16 May 2017

REVISED
19 July 2017

ACCEPTED FOR PUBLICATION
21 August 2017

PUBLISHED
28 September 2017

Keywords: inkjet printing, organic field effect transistors, polymeric insulator, access resistance, drop on demand

Supplementary material for this article is available online

Abstract

This study reports on the impact of electrodes (source and drain) and the insulator cross-sectional profile on the electrical behavior of printed organic field effect transistors (OFETs). Varying processing techniques, from classical lithography to inkjet printing, show different cross-sectional profiles. Indeed, due to the coffee stain effect (usually considered a drawback), the inkjet-printed insulator shows a wave-shaped profile although the spin-coated one is perfectly smooth. However, OFET electrical behavior is not drastically impacted by the insulator cross-sectional profile. Moreover, this study clearly demonstrates that independently of the insulator cross-sectional profile, OFETs fabricated with printed electrodes show the worst electrical characteristics. Consequently, this work clearly demonstrates that a challenging issue for the fabrication of efficient fully-printed OFETs relies on drain and source optimization (for instance, morphology or material).

Printed electronics (PE) has gained growing interest throughout the past decade [1]. Consequently, many techniques such as screen printing [2], roll to roll [3], inkjet printing [4–6], etc, have been considered. One of them, the drop on demand (DoD) inkjet printing technique, allows a very small amount of liquid deposition (1–100 pl) at high throughput and high accuracy on various kinds of substrates [1]. Moreover, DoD technology benefits from material deposition only at the desired location (i.e. maskeless additive patterning), reducing material consumption compared to the lithography technique (i.e. patterns fabricated using masks and the etching process). Those interesting properties will promote organic electronic production on non-conventional substrates such as flexible or biodegradable substrates. Indeed, most organic electronic devices such as organic light emitting diodes [7], solar cells [8] and organic field effect transistors (OFETs) [9, 10] can be fabricated using functional printable ink.

Inkjet printing technology requires multi-disciplinary skills and consequently many challenging topics, such as (i) functional inks formulation [11], (ii) jetting optimization [12], (iii) fluid drying control [13], (iv) device fabrication and characterization, etc [10, 14]. All these challenges must be addressed before the reliable fabrication of fully-printed devices. Thus, literature is replete with experimental works dealing with OFET electrical characteristics improvements using inkjet printing technology. In most cases, works focus on: new printable materials (i.e. organic semiconductors (OSC), insulators, conductive) [15–17], new semiconductor crystallization process [18], etc, and experiments are often performed on non-fully-printed OFET structures (smooth insulator and/or drain and source electrodes fabricated using the lithography technique) which offers better morphological characteristics than fully-printed ones. These studies are necessary but have to be completed with others dealing with deeper investigations on fully-printed OFET structures themselves.

A relevant study has highlighted the morphological impact of printed gate electrodes in bottom gate-bottom contact OFETs. It has been shown that the optimization of the gate electrodes profile (i.e. from convex to concave) strongly reduces OFET leakage current (I_G) [20]. This study has paved the way to

others, which have to report on the morphological impact of the other layers (insulator and/or source and drain electrodes) on OFET electrical behavior. Consequently, in this work and for the first time, the effect of a smooth polymeric insulator and a wave-shaped printed insulator on OFET electrical behavior have been studied. Such systematic study has been performed using printed silver as drain and source electrodes in the first section and thermally evaporated gold in the second one. Note that these materials have been chosen according to the literature. Indeed, silver and gold are the most frequently reported materials using inkjet printing and thermal evaporation, respectively.

Methods

Inks processing

Inks composition

Inks were used without filtering steps. Epoxy-based ink (Su8-2000 series; MicroChem, Westborough©, MA, USA) surface tensions and viscosity were 35 $mN.m^{-1}$ and 2.49 cp respectively. Silver nanoparticules (Silverjet DGP 40LT-15C from ANP©) surface tension and viscosity were 35 $mN.m^{-1}$ and 15 cp respectively.

Jettable criterion

The stroboscopic vision system was used to monitor the following criterion. The jettable criterion is the ability to obtain a droplet at a distance range (Δr) between 800 μm and 1 mm (acceptable working distance for the printer equipment: CERADROP© X-series). Satellite droplets or tails must be reabsorbed by the nozzle and jettability must be stable for a long time with low droplet misalignment on the substrate ($\Delta x < 5$ μm). All the measurements were performed at 1 KHz and 3 kHz jetting frequency for epoxy-based ink and silver based ink, respectively. Movies S1 and S2 (see supplementary files) show satisfying and unsatisfying jetting conditions, respectively.

OFET fabrication steps

All the printing experiments were performed using CERADROP© X-series printer.

Except the organic semiconducting layer, the OFET devices were fully printed on Corning© glass substrate.

The substrates were ultrasonically cleaned in acetone and isopropyl alcohol for 10 min. The silver gate electrode was printed on glass substrate using 256 nozzles Q-class printhead (Dimatix©) and baked on a hot plate at 130 °C for 30 min. Then, epoxy-based ink was printed using a 16-nozzle cartridge (Dimatix©) and baked at 95 °C for 5 min in an oven followed by UV ($\lambda = 365$ nm) exposure and baked again in an oven at 95 °C for 5 min. Due to the high hydrophobicity of the insulator, UV−ozone treatment (Jetlight©) is needed to increase its hydrophilicity, allowing the fabrication of accurate drain-source electrodes. Silver source and drain electrodes were printed on a 700 nm high epoxy layer. Finally, a 35 nm thick organic semiconductor (fullerene C60 Sigma Aldrich©) was thermally evaporated as an active layer.

Characterization

Viscosity and surface tension measurements were monitored using Malvern© labpro + rheometer and Kruss© DSA30 equipment, respectively. Profilometry measurements were performed using TENCOR© KLA P6 equipment. Optical pictures were obtained using a binocular vision system equipped with a camera (moticam©). All the electrical tests were performed inside a glovebox using Keithley© 2636A and Labview software.

Results and discussion

The DoD inkjet printing technique is based on the coalescence of printed droplets usually composed of solvent and solute (e.g. nanoparticles, polymers, etc) to form complex patterns after drying. As extensively described since the Deegan observations [19], a droplet of liquid is subject to the well-known phenomenon called the 'coffee stain effect' which results from greater evaporation rates at the surrounding of the 'triple contact line'. Consequently, when the triple line is pinned, solute transport from the center to the edge is induced by the replenish flow. This mechanism leads to non-uniform film morphology after complete solvent evaporation. Reducing the coffee stain effect is still a challenge to overcome in the field of DoD technology. Indeed, it requires complex (i) techniques development [20, 21], (ii) ink formulation [10, 22], (iii) printing parameters optimization [10] etc in order to obtain a profile which is as smooth as possible. Moreover, as the OFET is a multi-layer printed structure, it seems evident that each layer will induce additional disturbances during the drying step. Consequently, questions have to be answered: what is the impact of drying interactions between stacked layers on OFET electrical characteristics? Is it mandatory to perform a smooth insulator profile in order to fabricate electrically efficient fully-printed OFETs? Which layer (insulator or electrodes) is the key parameter impacting OFET electrical behavior? Note that the last two questions are particularly crucial for bottom-gate OFETs.

In order to determine such impacts, comparative studies have been performed between insulating films that are spin-coated or inkjet-printed.

Inkjet-printed source and drain electrodes

Processing and morphological study

As shown in figure 1 and more detailed in the experimental section, the bottom gate-bottom contacts

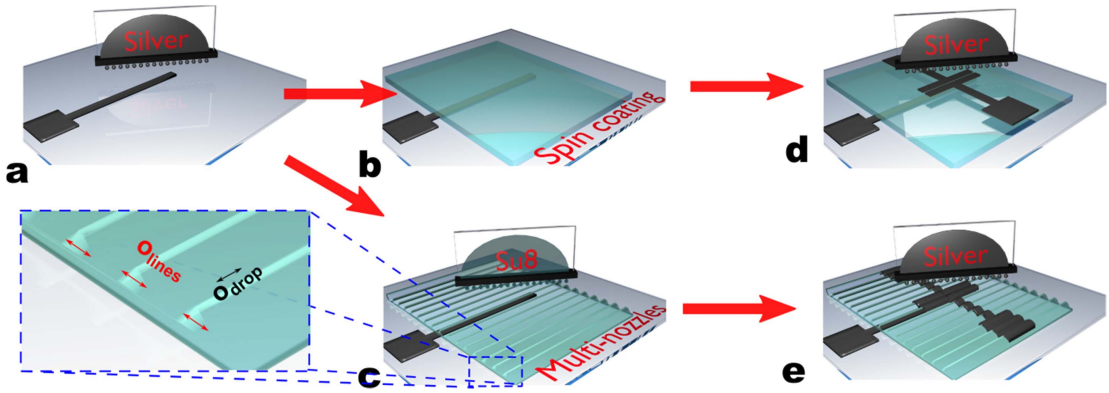

Figure 1. OFET fabrication steps including the variant steps for insulator fabrication. (a) Gate inkjet printing using silver nanoparticle-based ink, (b) spin-coating insulator (Su8-2000.5 photoresist), (c) inkjet-printed insulator (Su8-2000.5-based ink), (d) inkjet-printed source and drain electrodes (silver) on spin-coated insulator, (e) inkjet-printed source and drain electrodes (silver) on inkjet-printed insulator. Note that only the insulator profile varies for this set of experiments.

structure has been used to fabricate transistors in order to answer the previously mentioned questions. Insulator process variants (spin-coated or printed insulator) have been performed in order to highlight whether insulator processing techniques have a strong impact on OFET fabrication and electrical behaviors. Process variants are shown in figure 1 and can be described as follows.

Gate electrodes have been inkjet-printed using silver ink for all OFETs (figure 1(a)). As the effects of this step have already been extensively studied [20], the gate process was not changed in this study. After this step, the insulator has been performed using two different techniques: spin coating (figure 1(b)) and inkjet printing (figure 1(c)). The epoxy-based photoresist (Su8-2000 series; MicroChem, Westborough©, MA, USA) has been used as insulator because it has already demonstrated interesting insulating properties in many applications independently of fabrication techniques such as deep coating, spin coating and inkjet printing [10, 28, 29]. Moreover, epoxy-based insulators show low temperature processing (i.e. $<100\,^{\circ}C$), good chemical resistance, low leakage current density, a dielectric constant of about 3 [10, 28], high breakdown electric field (evaluated at $3\,mV.cm^{-1}$) and interesting wetting behavior. Indeed the hydrophobicity of insulator influences the OFET electrical behavior as demonstrated in [30] where the more the hydrophobicity was, the more the field effect value was.

The inkjet-printing insulator requires more experimental parameters adjustment than the spin-coated one. Indeed, DoD technology needs much more parameter optimization than spin coating. Both techniques need accurate control of the substrate temperature. However, DoD processing is particularly dependent on the (i) nozzle size, (ii) number of nozzles used at the same time during printing, (iii) jetting frequency, (iv) jetting waveform (see figure S1 available online at stacks.iop.org/FPE/2/035008/mmedia), (v) drops overlapping, etc. Here, the substrate temperature, nozzle size, activated nozzle number and jetting frequency have been kept constant at $50\,^{\circ}C$, 21 μm, 16 and 1 KHz, respectively. Jetting parameters are detailed in the supplementary file (see figure S1) and have also been kept constant. Those parameters have been experimentally optimized in order to respect jettable criterions (see experimental section) and perfect droplet printing behavior has been obtained (see movie S1) [10, 12]. Moreover, epoxy-based ink has also been used for its versatility because it is a low-molecular-weight based ink (7 KDa). Indeed, this ink can easily be printed without well-known jetting drawbacks (e.g. satellite droplets, long lived filaments, etc) as shown in movie S1 [10]. Note that ink composition and rheological parameters are detailed in the experimental section. Overlapping parameters will be discussed in depth in the following section.

As shown in figures 1(d) and (e), source and drain electrodes have been inkjet-printed for both insulator configurations. Fullerene (C60) has been chosen as a semiconductor because it is an extensively studied material giving relatively high field effect mobility [31] and because it allows one to fabricate N-type OFETs that are less studied in the literature. In the field of PE, the fabrication of fully-printed transistors as well as circuits is the ultimate goal. However, it is well known that transistors fabricated using solution-processed semiconductors often show less accurate results (i.e. more electrical characteristics dispersions) than evaporated ones. Indeed, using solution-processed semiconductors, crystals did not grow in the same direction, leading to an increase in the dispersion of OFET electrical characteristics. Those statements justify using thermally evaporated semiconductors in order to accurately study the transistor electrical behavior in the function of insulator morphologies and drain-source electrodes processing techniques.

As shown in figures 1(b), (c) and in figure 2, two different insulator morphologies have been performed. As published in another work [20], a smooth insulator surface has been obtained using the spin

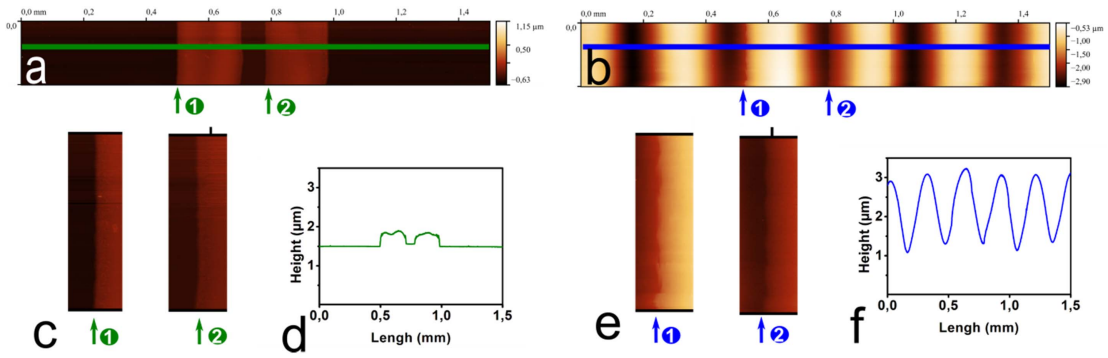

Figure 2. Morphological behavior of spin-coated devices and inkjet-printed devices. Top view scan (1.5 mm*200 μm) of drain and source electrodes fabricated on: (a) spin-coated Su8 insulator and (b) inkjet-printed Su8; (c) zoom on spin-coated insulator showing left side of inkjet-printed drain and source electrodes which are marked 1 and 2, respectively; (d) cross section along *x* axis of drain-source electrodes fabricated on spin-coated insulator; (e) zoom on inkjet-printed insulator showing left side of inkjet-printed drain and source electrodes which are marked 1 and 2, respectively; (f) cross section along *x* axis of drain-source electrodes fabricated on inkjet-printed insulator. Note that 3D profiles of printed layers are shown in figure S2(b).

coating technique onto printed gate (figures 2(a) and (d)). In this case, the centrifugal force induces a fast drying time that avoids the impact of the printed gate profile on insulator morphology. Moreover, well defined sources and drain electrodes (figures 2(c) and (d)) have been fabricated on spin-coated Su8 exposed to UV-ozone (see experimental section).

The printed insulator shows a wave-shaped profile mainly due to the coffee stain effect (figures 2(b) and (f)). This phenomenon has been extensively explained in a previous study and can be briefly summarized as follows [10]. Droplet coalescence along the *x* axis forms one line and line coalescence along the *y* axis forms the film. The lines are formed independently of each other and the evolution of the wavy shaped profile is due to the local coffee ring effect. The height of the peaks and valley are mainly governed by overlapping distance (O_{lines}) between adjacent lines (zoom in figure 1(c)) and by overlapping distance (O_{drop}) between adjacent droplets.

Concerning the drain and source electrodes, results reported in figure 2 contrast with previous studies that have shown a dewetting effect of printed material on top of wavy structures [32–34]. Indeed, the results of figures 2(b), (e), (f) and OFET optical pictures (see figure S2 in supplementary file) show that even if insulator profiles are strongly buckled (i.e. more than 2 μm height between the maximum and minimum values) drain-source electrodes are well defined (3D profiles are shown in figure S2). It signifies that chemically modified (OH groups appear due to UV-Ozone exposure) epoxy thin film offers the possibility to pin inkjet-printed silver ink. These results can be explained by the high contact-angle hysteresis value of epoxy thin film exposed to UV-ozone.

Electrical study

Figure 3 shows the transfer characteristics of OFETs using a spin-coated or inkjet-printed insulator. Moreover, relevant electrical parameters are summarized in table 1. Data shown in figure 3(a) is relative to spin-coated devices and figure 3(b) is relative to inkjet-printed devices. V_{GS} has been swept from −20 to 60 V with $V_{DS} = 20$ V. Figures show the transfer characteristics of five same-size OFETS fabricated on the same substrate. The common channel length L and width W are equal to 100 μm and 5000 μm, respectively. For each transistor, the subthreshold slope (SS) is calculated from the invert of the maximum slope of the drain current in logarithm scale as a function of the gate voltage in the subthreshold regime. The threshold voltage (V_{TH}) and the field effect mobility are calculated using the Y-function method established for silicon MOSFETs [35]. It has been established as a simple but powerful method to calculate low-field effect mobility, threshold voltage and contact resistance.

Main electrical parameters calculated using the Y-function method (detailed in supplementary file) are summarized in table 1 in order to compare the effect of insulator processing techniques (spin-coated or inkjet-printed). The results, depicted in table 1, do not show a clear tendency between the following electrical parameters: threshold voltage, subthreshold slope and contact resistances. Note that the intrinsic mobility μ_0 seems a little higher for spin-coated insulator, which could be correlated to the smoother insulator surface (see figure S3). In conclusion, the global OFET behavior is not strongly dependent of insulator processing techniques. It signifies that, even if buckled insulator profile occurs (see in figure 2) using inkjet printing technology, it does not drastically impact electrical OFET behavior.

The other parameter to check is the gate leakage current that cannot be negligible when using organic insulators and not silicon dioxide or alumina as usual. An original way to study the gate leakage is to make a zoom on the starting output characteristics of the OFETs at low values of the drain-source voltage V_{DS}.

At very low V_{DS}, the drain current starts from negative values for N-type OFETs as shown in figures 3(a) and (b) where the output characteristics

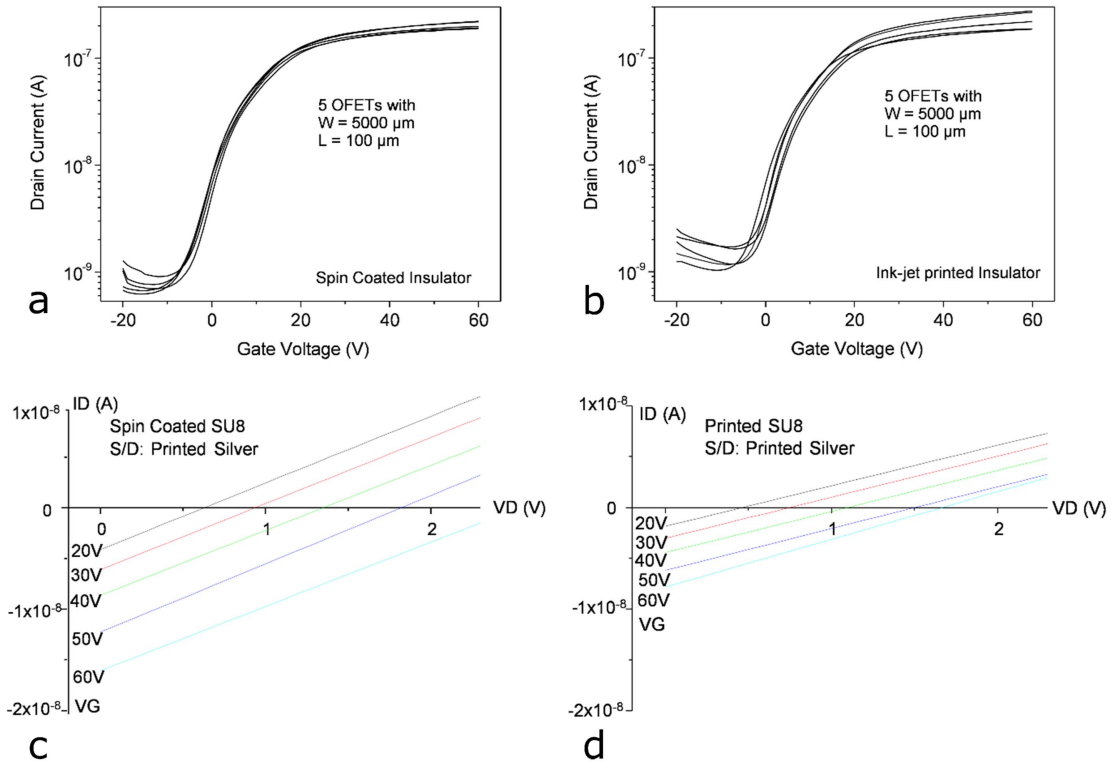

Figure 3. OFET transfer characteristics as a function of insulator fabrication with inkjet-printed source and drain electrodes. Transfer characteristics of five devices for: (a) spin-coated insulator, (b) inkjet-printed insulator. Output characteristics at low values of the drain-source voltage V_{DS} of OFETS for (c) spin-coated Su8 and printed source and drain electrodes; (d) printed Su8 and printed source and drain electrodes.

Table 1. Summary of electrical parameters as a function of insulator processing techniques (spin coating and inkjet printing). Note that source and drain contacts are inkjet-printed silver. μ_0, V_{TH}, SS and contact resistance R_c are calculated using the Y-function method.

Processing technique		W/L (μm/μm)	Insulator thickness in μm	μ_0 ($cm^2.V^{-1}.s^{-1}$)	V_{TH} (V)	SS (V/dec.)	R_C (Ω)	V_{DS} (V)
Spin	Average	5000/100	1.5	$1.2^{*}10^{-2}$	8	6.5	$6.5^{*}10^{7}$	20
	Stand. dev.	—	—	$4^{*}10^{-3}$	1.2	0.3	$2^{*}10^{7}$	—
IJP	Average	5000/100	1.7	$7.4^{*}10^{-3}$	9	6.5	$6.9^{*}10^{7}$	20
	Stand. dev.	—	—	$2^{*}10^{-3}$	2.8	0.2	$1.8^{*}10^{7}$	—

are plotted at very low V_{DS} values for the two types of OFETs. The starting negative value of the drain current I_D is more and more negative when the gate voltage V_{GS} is more and more positive. For the same value of V_{GS}, the starting value of I_D is more important for spin-coated SU8 OFETs than for printed SU8 ones.

Such behaviors are usual when the leakage current through the gate insulator is important. It can be explained considering the scheme of bottom-gate bottom contacts N-type OFET presented in figure 4.

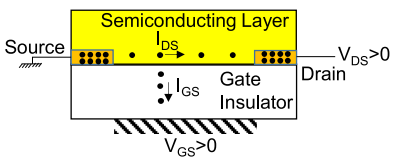

Figure 4. Scheme of N-type OFET showing the drain-source current I_{DS} and the gate-source current I_G.

At very low value of V_{DS}, the gate field due to V_{GS} is more important than the drain electric field due to V_{DS}. A high number of electrons flow in the direction of the positively polarized gate. Due to this important flow, electrons flow in the semiconductor to compensate the loss of electrons in the channel, inducing negative drain-source current. When V_{DS} increases, the drain-source electric field becomes more and more important inducing positive drain-source current. The V_{DS} value for which the drain current becomes positive occurs when the drain-source electric field becomes higher than the gate electric field.

Following such an explanation, the higher the starting negative value of I_D, the higher the gate leakage current for the same gate-source voltage. Figure 6 shows the starting negative drain current at V_{DS} closed

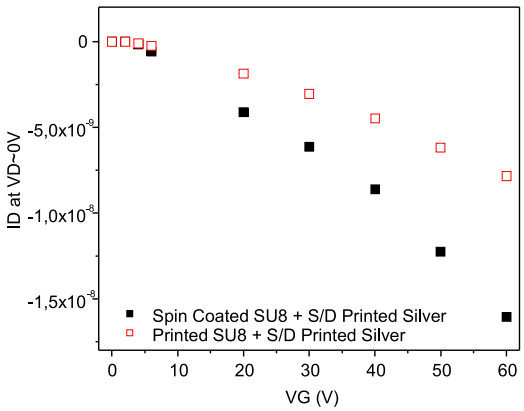

Figure 5. Starting negative drain current ($V_{DS} \sim 0$ V) as a function of gate-source voltage. This starting current is derived from the plot of output characteristics at different V_{GS}.

to 0 V as a function of the gate-source voltage for both types of OFETs. At very low gate-source voltage, drain current stays constant at around 0. This means that the gate electric field is not strong enough to induce gate leakage current. When the gate-source voltage is large enough to induce such leakage current, the starting drain current is negative. It is more and more negative when the gate-source voltage increases. For spin-coated SU8, the negative drain current starts to increase a little earlier than the current of printed SU8 and its value is higher when increasing V_{GS}. Gate leakage current is then slightly higher in spin-coated SU8. More precisely, it is difficult to determine the origin of this leakage. Indeed, it can be due to the intrinsic properties of the spin-coated SU8 and also to the use of printed silver as gate contact and as source/drain contact.

In conclusion, results have demonstrated that SU8 processing techniques do not show a high impact on OFET electrical behavior even if OFET fabricated using spin-coated Su8 as gate insulator induces more gate leakage current. These results show that the polymeric insulator fabricated using additive manufacturing techniques (e.g. IJP) is a good candidate in order to reach a fully solution-processed OFET. Indeed, with identical electrical behavior, there is no doubt that inkjet printing is mainly the most interesting technique for technological considerations. For instance, insulator deposition locally on the transistor gate will allow no electrical influence between transistors of the same circuits. Note that other inkjet printing advantages, such as low material consumption, have been previously described in the introduction section.

Evaporated gold film as source and drain electrodes

The results of the previous sections have shown moderate I_{on}/I_{off} ratio (approximately two decades), which is a limiting factor. Consequently, investigations have to be performed on drain and source contact processing techniques. In this section, thermally evaporated gold is used as a drain and source contact. Indeed, most of the relevant works dealing with non-fully solution-processed OFETs have been performed using thermally evaporated gold as a source and drain contact. Moreover, the same comparative study as in previous sections, focusing on insulator processing techniques, is performed.

As described previously, printed silver gate is performed and SU8 is deposited by spin coating or by printing (figures 6(b) and (c)). Then, source and drain electrodes (50 nm thick) are thermally evaporated (figures 6(d) and (e)).

Figure 7 shows the transfer characteristics of five OFETs (similar size: 5000 μm channel width and 100 μm channel length) using spin-coated SU8 or printed SU8. Table 2 shows the main OFET electrical parameters as function of insulator processing techniques.

Transfer characteristics clearly show that the I_{on}/I_{off} ratio equals at least six decades independently of processing techniques. Compare to previous results, the off-current is reduced and the on-current is increased by two decades and one decade, respectively. The low-field effect mobility increases, reaching 7×10^{-2} cm^2 V^{-1} s^{-1} for spin-coated SU8 OFETs as compared to the previous one (1×10^{-2} cm^2 V^{-1} s^{-1}). The subthreshold slope improves from 6.5 V/Dec to 3.5 V/Dec. Importantly, the contact resistance decreases by more than one decade.

If we check the leakage current by making, as previously, a zoom on the starting output characteristics of the OFETs at very low values of the drain-source voltage V_{DS} (figures 7(c) and (d)), we find the same negative drain current with more or less the same value if we compare the curves between figures 3 and 7. This means the gate leakage current in SU8 is similar. The difference occurs for the drain-source voltage values when drain current becomes positive. These values in figure 7 are much lower than in figures 3(a) and (b). Remembering this drain voltage occurs when the drain electric field is more efficient than the gate electric field, which means that the drain electric field is more efficient with evaporated source and drain contacts. It leads to higher drain current as expected from the higher value of the mobility and the lower value of the contact resistance.

This conclusion is confirmed by plotting the starting negative drain current closed to $V_{DS} = 0$ V as a function of the gate-source voltage for both types of OFETs. Comparing the curves in figures 5 and 8, we observe the starting drain current stays nearly 0, still a higher gate voltage for evaporated source/drain contact OFETs than for printed source/drain contact OFETs. This means we need higher gate-source voltage to compensate for the effect of the drain electric field and to get the starting negative drain current.

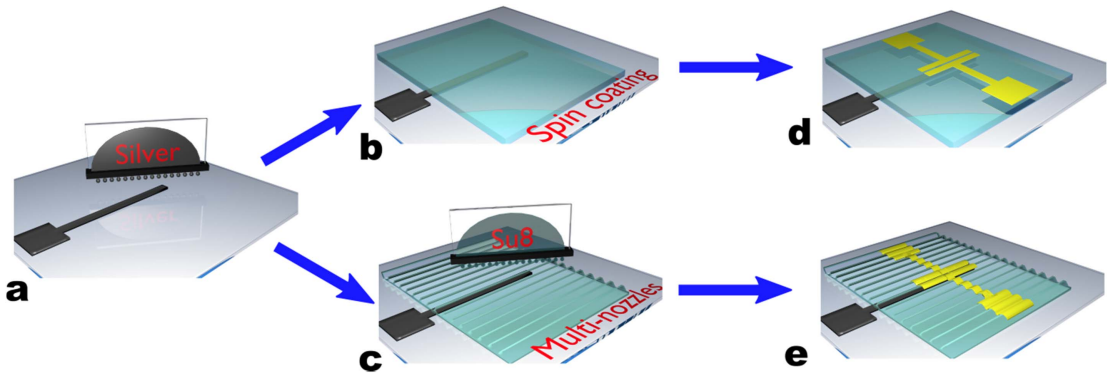

Figure 6. OFET fabrication steps including the variant steps for insulator fabrication. (a) Gate inkjet printing using silver nanoparticles based ink, (b) spin-coating insulator (Su8-2000.5 photoresist), (c) inkjet-printed insulator (Su8-2000.5-based ink), (d) source and drain electrodes (gold) thermally evaporated on spin-coated insulator and patterned using the lithographical process, (e) source and drain electrodes (gold) thermally evaporated on inkjet-printed insulator and patterned using lithographical process. Note that only the insulator profile varies for this set of experiments.

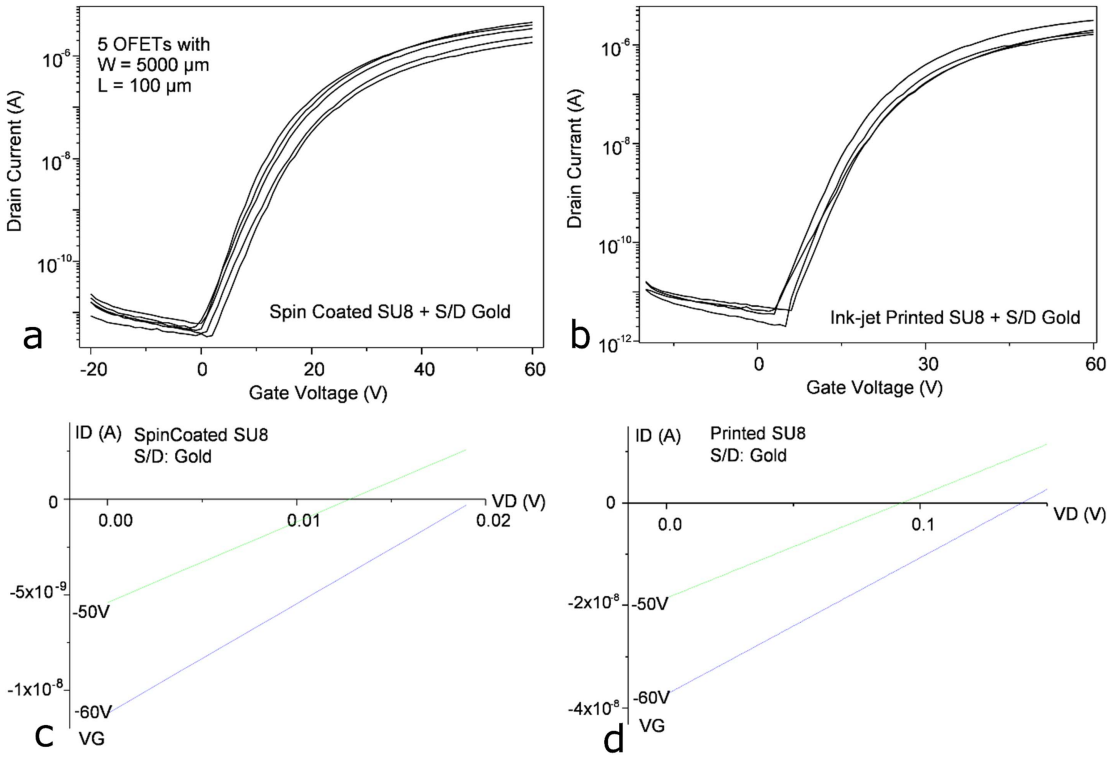

Figure 7. OFET transfer characteristics as a function of insulator fabrication with evaporated gold source and drain electrodes. (a) Transfer characteristics of five similar size devices for spin-coated insulator, (b) transfer characteristics of five devices for inkjet-printed insulator. Output characteristics at low values of the drain-source voltage V_{DS} of OFETS for (c) spin-coated Su8 and evaporated source and drain electrodes; (d) printed Su8 and evaporated source and drain electrodes.

Table 2. Represents the two insulator printing conditions (spin coating and inkjet printing) when source and drain contacts are gold evaporated. μ_0, V_{TH}, SS and contact resistance R_c are extracted from transfer characteristics using the Y-function method described in the text.

Processing technique		W/L (μm/μm)	Insulator thickness in μm	μ_0 ($cm^2.V^{-1}.s^{-1}$)	V_{TH} (V)	SS (V/dec.)	R_C (Ω)	V_{DS} (V)
Spin	Average	5000/100	1.5	$7^{*}10^{-2}$	29	3.6	$5.4^{*}10^{5}$	20
	Stand. dev.	—	—	$1.2^{*}10^{-2}$	3	0.2	$2.4^{*}10^{5}$	—
IJP	Average	5000/100	1.7	$3.8^{*}10^{-2}$	33	3.5	$2.1^{*}10^{6}$	20
	Stand. dev.	—	—	$0.6^{*}10^{-2}$	2.5	0.7	$2^{*}10^{6}$	—

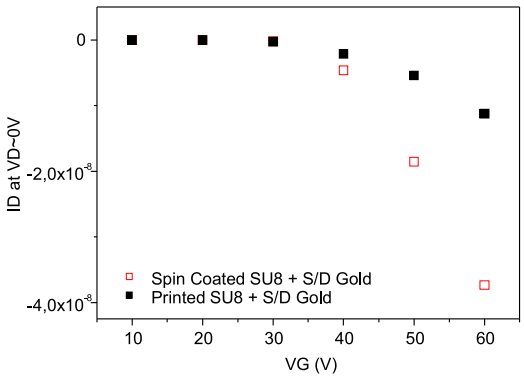

Figure 8. Starting negative drain current (at nearly 0 drain voltage) as a function of the gate voltage. This starting current is derived from the plot of output characteristics at a different gate voltage (figure 8).

Indeed, it is well known that in bottom contact structures, electrode engineering is one of the key parameters acting on charge injection into the OSC layer [36, 37]. In particular, thick electrodes disturb the continuous growth of a single-phase domain in the active layer [38]. Moreover, it has also been observed that thick electrodes can also induce high access resistance due to incomplete step coverage at the contact edge [39]. Note that drain and source material can also play a crucial role in OFET electrical behavior.

Conclusion

The ultimate goal of PE is to fabricate fully-printed devices and circuits. However, fully-printed OFETs usually show poorer electrical characteristics than evaporated ones. In this work, OFET structures have been investigated in order to highlight which layer(s) from the insulator and drain-source contacts layer have more effect on the electrical parameters. Here, we demonstrate that the insulator processing (spin coating or inkjet printing) technique is not the key parameter which drastically impacts the OFET electrical behavior. Indeed, the wave-shaped insulator profile, induced by the coffee ring effect and usually considered as a drawback, is not a limiting factor in order to achieve an efficient OFET. However, whatever the insulator deposition technique, the mobility and the on-off current ratio are lower and the contact resistance is higher when using printed source/drain contacts than when using evaporated source/drain contacts. Hypotheses can be drawn to explain this behavior such as: (i) the thickness and the morphological difference between printed and evaporated contacts, (ii) electrode materials. Consequently, such effects can be considered limiting factors for fully-printed OFET fabrication. This work has demonstrated that research has to focus on drain and source processing (thickness, morphology, new materials using new inks, etc) instead of insulator processing. Moreover, this work did not focus on fully-printed OFETs. Indeed, semiconductors must not be printed in order to avoid additional negative effects due to semiconductor drying. Obviously, such an effect remains challenging and has to be studied as in the impressive work performed by Minemawari *et al* [18].

References

[1] Calvert P 2001 *Chem. Mater.* **13** 3299–305
[2] Cho Y, Kim E and Kim W 2015 *Int. J. Technol. Manage.* **67** 106–31
[3] Pardo D A, Jabbour G E and Peyghambarian N 2000 *Adv. Mater.* **12** 1249–52
[4] Søndergaard R R, Hösel M and Krebs F C 2013 *J. Polym. Sci.* B **51** 16–34
[5] Derby B 2011 *J. Eur. Ceram. Soc.* **31** 2543–50
[6] Singh M, Haverinen H M, Dhagat P and Jabbour G E 2010 *Adv. Mater.* **22** 673
[7] Coenen M J, Slaats T M, Eggenhuisen T M and Groen P 2015 *Thin Solid Films* **583** 194–200
[8] Krebs F C 2009 *Sol. Energy Mater. Sol. Cells* **93** 394–412
[9] Medina-Sánchez M, Martnez-Domingo C, Ramon E and Merkoçi A 2014 *Adv. Funct. Mater.* **24** 6291–302
[10] Robin M, Kuai W, Amela-Cortes M, Cordier S, Molard Y, Mohammed-Brahim T, Jacques E and Harnois M 2015 *ACS Appl. Mater. Interfaces* **7** 21975–84
[11] Mionic M, Pataky K, Gaal R, Magrez A, Brugger J and Forró L 2012 *J. Mater. Chem.* **22** 14030–4
[12] Nallan H C, Sadie J A, Kitsomboonloha R, Volkman S K and Subramanian V 2014 *Langmuir* **30** 13470–7
[13] Derby B 2010 *Ann. Rev. Mater. Res.* **40** 395–414
[14] Sowade E, Mitra K Y, Ramon E, Martinez-Domingo C, Villani F, Loffredo F, Gomes H L and Baumann R R 2016 *Org. Electron.* **30** 237–46
[15] Gamerith S, Klug A, Scheiber H, Scherf U, Moderegger E and List E J 2007 *Adv. Funct. Mater.* **17** 3111–8
[16] Jeong S *et al* 2013 *J. Mater. Chem.* C **1** 2704–10
[17] Kim C, Wang Z, Choi H-J, Ha Y-G, Facchetti A and Marks T J 2008 *J. Am. Chem. Soc.* **130** 6867–78
[18] Minemawari H, Yamada T, Matsui H, Tsutsumi J, Haas S, Chiba R, Kumai R and Hasegawa T 2011 *Nature* **475** 364–7
[19] Deegan R D, Bakajin O, Dupont T F, Huber G, Nagel S R and Witten T A 1997 *Nature* **389** 827–9
[20] Fukuda K, Sekine T, Kumaki D and Tokito S 2013 *ACS Appl. Mater. Interfaces* **5** 3916–20
[21] Etxebarria I, Tait J, Gehlhaar R, Pacios R and Cheyns D 2013 *Org. Electron.* **14** 430–5
[22] Kim D, Jeong S, Park B K and Moon J 2006 *Appl. Phys. Lett.* **89** 264101
[23] Chang J, Zhang X, Ge T and Zhou J 2014 *Org. Electron.* **15** 701–10
[24] Kim J, Lim B, Baeg K-J, Noh Y-Y, Khim D, Jeong H-G, Yun J-M and Kim D-Y 2011 *Chem. Mater.* **23** 4663–5
[25] Ko S H, Pan H, Grigoropoulos C P, Luscombe C K, Fréchet J M and Poulikakos D 2007 *Nanotechnology* **18** 345202
[26] Kim B, Jang S, Geier M L, Prabhumirashi P L, Hersam M C and Dodabalapur A 2014 *Nano Lett.* **14** 3683–7
[27] Baeg K-J, Khim D, Kim D-Y, Jung S-W, Koo J B, You I-K, Yan H, Facchetti A and Noh Y-Y 2011 *J. Polym. Sci.* B **49** 62–7
[28] Dufour R, Dibao-Dina A, Harnois M, Tao X, Dufour C, Boukherroub R, Senez V and Thomy V 2013 *Soft Matter* **9** 492–7
[29] Jacques E, Romain M, Yassin A, Bebiche S, Harnois M, Mohammed-Brahim T, Rault-Berthelot J and Poriel C 2014 *J. Mater. Chem.* C **2** 3292–302
[30] Yang S Y, Shin K and Park C E 2005 *Adv. Funct. Mater.* **15** 1806–14
[31] Jian-Lin Z, Jun-Sheng Y, Xin-Ge Y and Xin-Yang C 2012 *Chin. Phys.* B **21** 027305

[32] Tseng H-Y and Subramanian V 2011 *Org. Electron.* **12** 249–56
[33] Sirringhaus H, Kawase T, Friend R, Shimoda T, Inbasekaran M, Wu W and Woo E 2000 *Science* **290** 2123–6
[34] Wang J, Zheng Z, Li H, Huck W and Sirringhaus H 2004 *Nat. Mater.* **3** 171–6
[35] Ghibaudo G 1988 *Electron. Lett.* **24** 543–5
[36] Xu Y, Minari T, Tsukagoshi K, Chroboczek J and Ghibaudo G 2010 *J. Appl. Phys.* **107** 114507
[37] Horowitz G 2011 *Open Appl. Phys. J.* **4** 2–7
[38] Xu M, Nakamura M, Sakai M and Kudo K 2007 *Adv. Mater.* **19** 371–5
[39] Richards T and Sirringhaus H 2007 *J. Appl. Phys.* **102** 094510